Laminar-Turbulent Transition in Swept-Wing Flows with a Supercritical Forward-Facing Step

Casacuberta, J.; Hickel, S.; Kotsonis, M.

DOI
10.1007/978-3-031-47028-8_23

Publication date
2024

Document Version
Final published version

Published in
ERCOFTAC Series

Laminar-Turbulent Transition in Swept-Wing Flows with a Supercritical Forward-Facing Step

J. Casacuberta(✉), S. Hickel, and M. Kotsonis

Aerodynamics Group, Faculty of Aerospace Engineering,
Delft University of Technology, Kluyverweg 1, 2629HS Delft, The Netherlands
J.CasacubertaPuig@tudelft.nl

1 Introduction

Achieving and maintaining laminar flow on large swept lifting surfaces of subsonic aircraft poses a considerable challenge. Surface roughness, such as imperfect joints introducing sharp surface distortions, is a source of significant laminar flow deterioration that promotes laminar-turbulent transition.

The present work considers a laminar-turbulent transition route initiated by primary (stationary crossflow) eigenmode amplification, which is the prevalent scenario in low-disturbance environments as in free-flight [9]. This instability kind manifests in the developed flow field as stationary co-rotating vortices whose axes of rotation are practically aligned with the direction of the streamlines in the outer-flow region. Under Decomposition (1), the developed flow $\mathbf{q} = [u\ v\ w\ p]^T$ is conceived as the superposition of the laminar unperturbed base flow, $\mathbf{q}_\mathrm{B}$, with steady, $\mathbf{q}'$, and unsteady, $\mathbf{q}''$, perturbation fields:

$$\mathbf{q}(x, y, z, t) = \mathbf{q}_\mathrm{B}(x, y) + \mathbf{q}'(x, y, z) + \mathbf{q}''(x, y, z, t). \tag{1}$$

In stationary-crossflow-dominated flows, forward-facing steps significantly altering the laminar-turbulent transition path may be classified as critical or supercritical. Critical steps advance the transition front upstream, as compared to a reference clean (i.e. no step present) case. Supercritical steps trip the flow immediately and have been found to drastically move the transition front to the vicinity of the step. The main goal of the present work is to investigate the step-flow mechanisms responsible for inducing a supercritical transition scenario. To this end, we carry out Direct Numerical Simulations (DNS) and perform a modal analysis of the steady and unsteady perturbation fields.

2 Flow Problem and DNS Setup

The incompressible swept-wing flow is modeled as flat-plate flow with an imposed airfoil-like pressure gradient in the chordwise direction at the free-stream. The main coordinate system reads $\mathbf{x} = [x\ y\ z]^T$, where x, y, z indicate the chordwise (i.e. normal to the virtual leading edge), wall-normal, and spanwise (i.e.

C. Marchioli et al. (Eds.): DLES 2023, ERCO 31, pp. 151–156, 2024.
https://doi.org/10.1007/978-3-031-47028-8_23

parallel to the virtual leading edge) directions, respectively. The coordinate $x_{\mathrm{st}} = x - 177.62\,\delta_0$ is additionally introduced to express the relative chordwise distance to the step. The inlet free-stream velocity is decomposed into a chordwise component, u_∞, and a spanwise component, $w_\infty = -1.24u_\infty$, to model the effect of sweep angle. Pressure measurements from wind-tunnel experiments on a 45° swept wing [7] are used to guide the DNS setup. The inflow boundary layer thickness, $\delta_0 = 7.71 \times 10^{-4}$ m, and free-stream velocity, $u_\infty = 15.10$ m/s, are chosen as global characteristic quantities.

A stationary crossflow mode, computed as solution to a local linear Orr-Sommerfeld analysis on the base flow profile, is prescribed at the inflow. The step height, $h = 0.97\delta_0$, corresponds to approximately 50% of the undisturbed boundary layer thickness at the virtual step location. The spanwise domain length (i.e. fundamental spanwise wavelength) is set to $\lambda_z = 7.5$ mm. This wavelength yields the integrally most amplified perturbation at the end of the computational domain in reference no-step conditions.

In Sects. 3 and 4, we will analyze steady and unsteady perturbation effects. The steady perturbation field, $\mathbf{q}'$, is decomposed in spanwise Fourier modes, i.e.

$$\mathbf{q}'(x, y, z) = \sum_{j=-N}^{N} \tilde{\mathbf{q}}_j(x, y) \mathrm{e}^{\mathrm{i}j\beta_0 z}, \tag{2}$$

where N is the number of modes considered, $\tilde{\mathbf{q}}_j$ is the Fourier coefficients of mode j, $\beta_0 = 2\pi/\lambda_z$, and $\mathrm{i}^2 = -1$.

The DNS of the incompressible Navier-Stokes equations are performed with INCA, a conservative finite-volume solver. The Navier-Stokes equations are marched in time with a third-order Runge-Kutta method. A fifth-order upwind scheme is used to discretize the convective terms. The Selective Frequency Damping (SFD) technique [1] is applied to numerically compute the stationary isolated form of $\mathbf{q}'$ following a recently proposed methodology to compute the control parameters [3].

The computational domain encompasses $0 \leq x/\delta_0 \leq 517$ and $y/\delta_0 \leq 26$ and the grid contains $N_x = 6760$, $N_y = 1008$, and $N_z = 144$ points in the chordwise, wall-normal, and spanwise directions, respectively. These values yield $\Delta x^+ = 1.8$, $\Delta y^+ = 0.9$, and $\Delta z^+ = 9$ in the steady perturbed flow (i.e. $\mathbf{q}_\mathrm{B} + \mathbf{q}'$) near the step. Numerical computations of the unperturbed base flow, $\mathbf{q}_\mathrm{B}$, and the steady perturbed flow, $\mathbf{q}'$, are performed independently for a similar numerical setup. In the former, the equations are converged in time up to a threshold value of 10^{-8} based on an L_2-norm of the temporal derivatives. In the latter, unsteady perturbation content is triggered by a multi-modal harmonic forcing of the wall-normal velocity at the wall near the inflow ($20 \leq x/\delta_0 \leq 32$) as follows:

$$v(x, 0, z, t) = f_s(x) \sum_{k=1}^{M} A_k^{\mathrm{BS}} \cos(\beta_0 z + 2\pi k f_0 t + \phi_k), \tag{3}$$

with f_0 representing a fundamental temporal frequency, A_k^{BS} indicates the initial amplitude of a temporal component k, ϕ_k is a random phase, and f_s modulates

smoothly the response in x. Unsteady forcing is applied ranging from 3 kHz to 14 kHz in intervals of 1 kHz. For the present setup, the DNS results reproduce the transitional-flow scenario observed in experiments in a low-disturbance wind tunnel [7].

3 Steady Perturbation Evolution

To elucidate on the modification of the transition path by the step, the evolution of the steady perturbation field ($\mathbf{q}'$) is first addressed. An overview of the subsequent unsteady flow evolution and the ultimate transition mechanisms will be discussed in the next section.

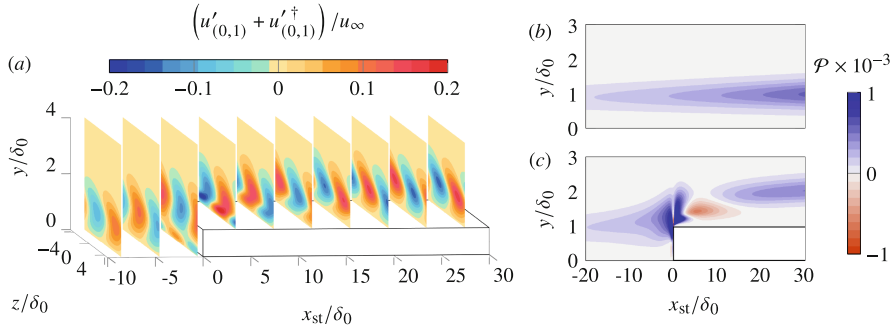

Fig. 1. Evolution of the fundamental perturbation Fourier mode at the step (a). Spatial evolution of linear energy production for $\beta = \beta_0$ in the no-step (b) and step (c) cases.

Around the step, two major flow regimes are identified. *Far* from the wall, the pre-existing crossflow perturbation lifts off and passes over the step. *Close* to the wall, chordwise-velocity (u') perturbation streaks of alternating sign in z are induced at the step apex (Fig. 1(a)). This scenario develops analogously for each Fourier mode, implying that a near-wall streak system contained in a particular Fourier mode *has adopted* the spanwise wavelength of the incoming crossflow component that induces it.

The origin and evolution of such new streaky structures induced at the step is scrutinised next by formulating energy-balance equations of the spanwise-harmonic perturbation modes [5]. They read

$$0 = \mathcal{P}_{n\beta_0} + \mathcal{T}_{n\beta_0} + \mathcal{D}_{n\beta_0} + \mathcal{W}_{n\beta_0} + \mathcal{N}_{n\beta_0}, \; n = 0, 1, \ldots, N, \tag{4}$$

where $\mathcal{P}_{n\beta_0}$ denotes linear energy production, $\mathcal{T}_{n\beta_0}$ is the advection of perturbation kinetic energy by the base flow, and $\mathcal{D}_{n\beta_0}$, $\mathcal{W}_{n\beta_0}$, $\mathcal{N}_{n\beta_0}$ express the work done by viscous forces, pressure forces, and non-linear perturbation interactions, respectively.

In essence, Eq. (4) expresses a balance between different perturbation mechanisms which remain in temporal equilibrium. The balance is harmonic, implying that it accounts for perturbation mechanisms acting on a particular perturbation Fourier space $n\beta$, solely. Equation (4) reduces to the well-known Reynolds-Orr equation under certain flow conditions.

When the budget analysis based on Eq. (4) is applied to the fundamental perturbation field, $\beta = \beta_0$, it is found that linear production ($\mathcal{P}_{\beta_0}$) is the dominant perturbation mechanism in both the near- and far-wall regimes. Similar results have been reported recently by use of stability tools applied on the step flow [4]. In particular, the spatial evolution of the dominant term $\mathcal{P}_{\beta_0}$ is portrayed in Fig. 1(*b*,*c*). The enhanced blue region with $\mathcal{P}_{\beta_0} > 0$ around the step is associated to the mechanism responsible for inducing streaks; essentially, it expresses that kinetic energy is transferred from the base flow to the perturbation field. At the same time, in the region further from the wall, an algebraic instability associated to the lift-up effect is proposed as a main mechanism responsible for the (linearly-dominated) alteration of the fundamental crossflow perturbation at the step. This is elaborated upon in an article in preparation [6].

When the initial amplitude of the pre-existing crossflow instability is sufficiently small, the near-wall streaks vanish rapidly downstream of the step (Fig. 1(*a*)). This is observed for a choice of amplitude of the pre-existing instability that yields linear behaviour until the virtual step location in reference conditions (i.e. without the step). By the increase of the amplitude of the incoming instability, it is observed that, eventually, the perturbation streaks originally induced at the step apex are sustained in space and amplified in x. By evaluating the relative contribution of the terms of Eq. (4), this is ascribed to the work of non-linear interactions between perturbation streaks among all harmonic spaces, i.e. for $\beta = \beta_0$ as well as for $\beta > \beta_0$. This (non-linear) growth of perturbation streaks close downstream of the step plays a main role in significantly deforming both, the shear layer close to the wall and the topology of the incoming stationary crossflow vortex.

4 Unsteady Perturbation Evolution

For the presently investigated step height, laminar-turbulent transition is captured shortly downstream of the step. This is line with observations of recent experimental investigations [7] under similar flow conditions and step geometry. The results of our DNS indicate that the shear layer significantly deformed by the step is prone to unsteady perturbation amplification. The explosive chordwise growth of unsteady perturbation structures downstream of the step initiates the breakdown of the laminar flow. Following the discussion in the previous section, the occurrence of supercritical transition appears to be exclusive to cases with a sufficiently large pre-existing stationary crossflow perturbation.

Figure 2 depicts an instantaneous isosurface of the Q-criterion for the unsteady developed flow. Close downstream of the step, wedges of unsteady contamination approximately aligned with the crossflow-vortex direction are the

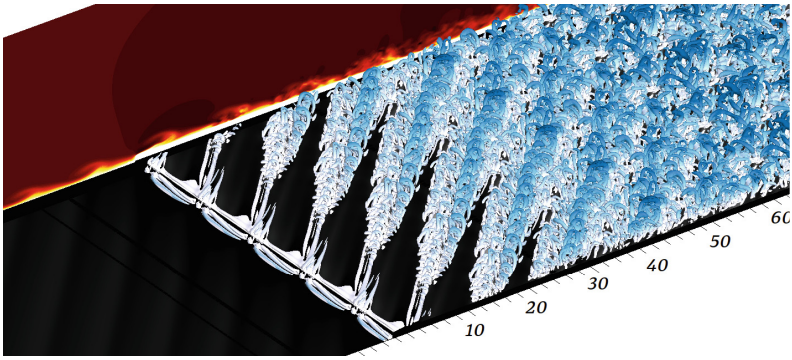

Fig. 2. Instantaneous Q-criterion isosurface colored by wall distance (white indicates close to the wall) and x-y plane of instantaneous chordwise-velocity. The x_{st}-axis is expressed in units of δ_0.

precursor of turbulence. Even though the unsteady fluctuations arise rather close to the wall, they manifest at significantly larger frequencies than those associated typically to the *type*-III secondary crossflow instability. The latter has been reported as well in corresponding experimental investigations [8] for a similar setdup. This finding suggests that a new transition mechanism is introduced by the step; it would effectively by-pass the growth of the secondary crossflow instabilities, which induce typically the breakdown of the stationary crossflow vortices in reference no-step conditions.

It is noted that the unsteady fluctuations initiating the laminar breakdown process develop in the shear layers embedding the stationary streaks induced at the step apex. In particular, two main families of large-scale hairpin vortices are captured in the DNS driving the unsteady wedges. The origin of both families of hairpin vortices is found at the upper part of regions of low-speed streaks. Accordingly, in future work it will be investigated whether the unsteady structures responsible for inducing supercritical transition by a forward-facing step are related to the so-called varicose and sinuous instabilities [2]; these develop typically in streaky boundary-layer flows subject to high levels of free-stream turbulence in scenarios of classic by-pass transition.

References

1. Åkervik, E., Brandt, L., Henningson, D.S., Hoepffner, J., Marxen, O., Schlatter, P.: Steady solutions of the Navier-Stokes equations by selective frequency damping. Phys. Fluids **18**, 068102 (2006)
2. Brandt, L.: Numerical studies of the instability and breakdown of a boundary-layer low-speed streak. Eur. J. Mech. B/Fluids **26**, 64–82 (2007)
3. Casacuberta, J., Groot, K.J., Tol, H.J., Hickel, S.: Effectivity and efficiency of selective frequency damping for the computation of unstable steady-state solutions. J. Comput. Phys. **375**, 481–497 (2018)

4. Casacuberta, J., Hickel, S., Westerbeek, S., Kotsonis, M.: Direct numerical simulation of interaction between a stationary crossflow instability and forward-facing steps. J. Fluid Mech. **943**, A46 (2022)
5. Casacuberta, J., Hickel, S., Kotsonis, M.: Laminar-turbulent transition by crossflow instability interacting with forward-facing step: direct numerical simulations. Manuscript in preparation
6. Casacuberta, J., Hickel, S., Kotsonis, M.: Passive stabilization of crossflow instabilities by a reverse lift-up effect. Manuscript in preparation
7. Rius-Vidales, A.F., Kotsonis, M.: Impact of a forward-facing step on the development of crossflow instability. J. Fluid Mech. **924**, A34 (2021)
8. Rius-Vidales, A.F., Kotsonis, M.: Unsteady interaction of crossflow instability with a forward-facing step. J. Fluid Mech. **939**, A19 (2022)
9. Saric, W.S., Reed, H.L., White, E.B.: Stability and transition of three-dimensional boundary layers. Annu. Rev. Fluid Mech. **35**, 413–440 (2003)